VLES turbulence model for an Eulerian-Lagrangian modelling concept for bubble plumes

Jan Erik Olsen*, Paal Skjetne, Stein Tore Johansen

SINTEF Materials & Chemistry, 7465 Trondheim, NORWAY
*Corresponding author, E-mail address: Jan.E.Olsen@sintef.no

ABSTRACT

Traditional Reynolds-averaged Navier-Stokes (RANS) approaches to turbulence modelling, such as the k-ϵ model, have some well-known shortcomings when modelling transient flow phenomena. To mitigate this, a filtered URANS model has been derived where turbulent structures larger than a given filter size (typically grid size) is captured by the flow equations and smaller structures are modelled according to a modified k-ϵ model. This modelling approach is also known as a VLES model (Very Large Eddy Scale model), and provides more details of the transient turbulence than the k-ϵ model at little extra computational cost.

In this study a two-phase extension to the VLES model is described. A modelling concept for bubble plumes has been developed in which the bubbles are tracked as particles and the flow of liquid is solved by the Navier-Stokes equations in a traditional mesh based approach. The flow of bubbles and liquid is coupled in an Eulerian-Lagrangian model. Turbulent dispersion of the bubbles is treated by a random walk model. The random walk model depends on an estimation of the eddy life time. The eddy life time for the VLES model differs from a k-ϵ model, and its mathematical expression is derived.

The model is applied to ocean plumes emanating from discharge of gas at the ocean floor. Validation with experiments and comparison with k-ϵ model are shown.

Keywords: bubble, plume, turbulence, VLES, CFD, Lagrangian

1 INTRODUCTION

Bubble plumes are found in various industrial processes, in coastal and harbour facilities and in natural and accidental subsea discharges. Accurate mathematical predictions of their behaviour enable cost effective process optimization and reliable risk assessments.

Mathematical modelling of bubble plumes was initiated before WWII [1][1] when classical models for buoyant plumes were developed. Later these models was enhanced by implementing more relevant physics including gas expansion, two phase effects and gas dissolution. The models assume a profile (typically Gaussian) for the vertical velocity and the volume fraction of bubbles. By integrating the conservation equations for mass and momentum in the radial direction with the assumed profile, a one dimensional (1D) set of equations is derived. These models are therefore also known as integral models.

During the 1980's, CFD became an applicable tool for two-phase flows which enabled modelling of bubble plumes. Schwarz and Turner [2] developed an Eulerian-Eulerian model for bubble plumes in metal reactors. Eulerian-Lagrangian algorithms were also developed in the 1980's. Johansen and Boysan [3] published an axisymmetric model for bubble plumes in reactors. It has been argued that in three dimensions (3D) and for relevant gas release rates, Lagrangian tracking of the resulting number of bubbles is very demanding on computer resources, and thus an Eulerian-Eulerian approach is preferable for bubble plumes with a huge quantity of bubbles. Swan and Moros [4] solved this issue for the Lagrangian approach by tracking groups of bubbles instead of individual bubbles. They adopted the technique in an axisymmetric model for subsea blowouts similar to the modelling concept of Johansen and Boysan [3].

Cloete, Olsen and Skjetne [5] documented that full 3D modelling of large scale bubble plumes with an Eulerian-Lagrangian approach was possible and that the modelling concept was consistent pool experiments. The Eulerian-Lagrangian modelling concept is based on a VOF (volume of fluid) model for capturing the flow in the continuous phases and the interphase between the continuous phases, and a discrete phase model, DPM, for tracking the bubble motion. The bubbles are tracked in parcels representing many bubbles (or particles) where all bubbles share the same properties similar to Swan and Moros [4]. Thus the VOF-DPM approach is computationally affordable.

Most of these two-phase models deploy a k-ϵ model for quantifying the turbulence in the flow. The model is robust and computationally affordable, but is known to fail on predictions related to transient behavior (e.g. vortex shedding behind a cylinder [5]) and swirling (e.g. cyclones [6]). The LES model is better suited for transient flow. Several authors [7-10] have compared the performance of the LES and k-ϵ model and various closure laws for drag and other interfacial forces in bubbly flows. They typically account for buoyancy, drag, lift, virtual mass, bubble induced turbulence and turbulent dispersion. However, some [10, 11] do not account for turbulent dispersion and may thus wrongly interpret the effect of some of the other forces. Regardless of this, all conclude that LES is more reliable for turbulence modelling than the k-ϵ model.

Most of the above mentioned results stem from simulations and experiments performed on lab-scale bubble columns. When considering large scale bubble plumes, e.g. full scale industrial reactors or bubble plumes in the ocean, the computational cost of running LES simulations can become substantial. Thus a more affordable modelling approach for turbulence in transient flows has been proposed which inherently captures the larger turbulent structures. It is known as a VLES model (very large eddy scale). In the following chapter we describe the Eulerian-Lagrangian modelling concept for bubble plumes and how a VLES model is coupled to the modelling concept. The novelty lies in the implementation of the VLES model into an existing modelling concept [12] which relied on the k-ϵ model for turbulence.

[1] The work was published later.

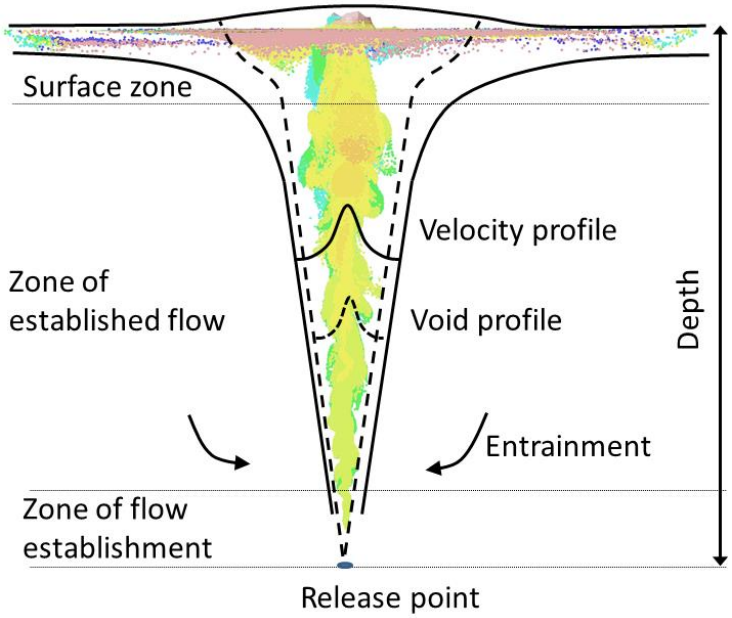

Figure 1: Bubble plume in ocean.

2 MODEL DESCRIPTION

The objective of a model for bubble plumes is to quantitatively predict bubble flow, liquid flow and (if requested) the flow of gas above the liquid. In a Lagrangian framework the bubbles move according to Newton's second law. The bubble acceleration is given by a force balance:

$$\frac{d\boldsymbol{u}_b}{dt} = \frac{\boldsymbol{g}(\rho_b - \rho)}{\rho_b} + \boldsymbol{F}_D + \boldsymbol{F}_{VM} \tag{1}$$

The first term on the right hand side is the specific buoyancy force (force divided by bubble mass). The other forces are drag and virtual mass force. The specific drag force is

$$\boldsymbol{F}_D = \frac{18\mu}{\rho_b d_b^2}\frac{C_D \mathrm{Re}}{24}(\boldsymbol{u}_b - \boldsymbol{u}) \tag{2}$$

where C_D is the drag coefficient, Re is the Reynolds number, ρ_b is the density of the bubble gas and d_b is the bubble diameter. The driving mechanism of the drag force is the velocity difference between the bubbles and the liquid $\boldsymbol{u}_b - \boldsymbol{u}$**.** Note that $\boldsymbol{u}$ is the instantaneous velocity of the background fluid

$$\boldsymbol{u} = \boldsymbol{U} + \boldsymbol{u}' \tag{3}$$

accounting for both the average velocity $\boldsymbol{U}$ and the turbulent fluctuations $\boldsymbol{u}'$**.** The turbulent fluctuations in the drag force cause turbulent dispersion. As in all models not resolving the turbulence, the turbulent dispersion is calculated by a sub-model. For Lagrangian tracking of bubbles (or particles) we apply a *random walk model* [13] in which the turbulent velocity fluctuations is calculated by

$$\boldsymbol{u}' = \boldsymbol{\xi}\sqrt{k} \tag{4}$$

if a k-ϵ turbulence model is deployed. Here $\boldsymbol{\xi}$ is a Gaussian distributed random number and k is the turbulent kinetic energy. The time of which this velocity fluctuation is applied in the integration of the bubble trajectory is limited by the eddy lifetime (or the time it takes for a bubble to traverse through a turbulent eddy). The eddy lifetime is

$$\tau_e = 0.15\frac{k}{\epsilon} \tag{5}$$

for a k-ϵ model. The drag coefficient is given by the expression of Tomiyama, Kataoka, Zun and Sakaguchi [14] for contaminated conditions with an adjustment ~~a correction~~ for bubble interactions at high volume fractions based on the work of Tsuji, Morikawa and Terashima [15].

Virtual mass force, also known as added mass force, is the force added to a bubble because an accelerating body is deflecting some volume of the surrounding fluid as it moves through it. The specific force is given as

$$\boldsymbol{F}_{VM} = C_{VM}\frac{\rho}{\rho_b}\left(\frac{D\boldsymbol{u}}{Dt} - \frac{d\boldsymbol{u}_b}{dt}\right) \tag{6}$$

where $C_{VM} = 0.5$ is the virtual mass coefficient. Lift force is normally included in reactor modelling of bubble plumes. However, there are uncertainties with respect to the lift coefficients in turbulent plumes. For single bubbles the correlation of Tomiyama, Tamai, Zun and Hozokawa [16] is well accepted, but for bubbles affected by neighboring bubbles few direct studies of the lift coefficient have been performed. Indirect studies has been conducted where the lift coefficient have been used as a tuning coefficient. Some of these studies (e.g. [11]) neglect turbulent dispersion and apply the lift coefficient as a means to add dispersion and overall spreading of the plume. This approach, neglecting fundamental physics, is not viable. The lift force is furthermore expected to be very sensitive to surfactants, available in natural water and brine. Since turbulent dispersion by drag is the major dispersion mechanism in bubble plumes, and there are too many open questions related to the lift coefficients, the lift force is currently neglected.

The bubbles are tracked as unstructured point particles without any direct interaction like collisions and intermediate pressure forces. Although the bubbles do not interact directly, they feel the presence of other bubbles through the interaction with the background fluid. This indirect interaction can be seen in the bubble size which accounts for coalescence and break up based on, among other, feedback on bubble volume fraction. The bubble size in dense plumes is assumed to be governed by turbulence break up and coalescence. In more dilute plumes mass transfer and gas expansion due to pressure gradients will dominate. A model for an Eulerian framework accounting for break up and coalescence was developed by Laux and Johansen [17]. When this model is recast into a Lagrangian framework with the effect of mass transfer and gas expansion included, the bubble size is given by the following differential equation

$$\dot{d}_b = \frac{d_b^{eq} - d_b}{\tau_{cb}} + \frac{d_b}{3}\left(\frac{\dot{m}_b}{m_b} - \frac{\dot{\rho}_b}{\rho_b}\right) \tag{7}$$

Here m_b is the mass of a bubble, $\dot{m}_b$ is the mass transfer rate from a bubble, $\dot{\rho}_b$ is the Lagrangian time derivative of the bubble density, τ_{cb} is the time scale for coalescence or break up and d_b^{eq} is the bubble diameter obtained by a bubble if it is exposed to given flow conditions (turbulent dissipation and plume density) for a sufficient time (i.e equilibrium is reached). This equilibrium bubble diameter is

$$d_b^{eq} = C_1\sqrt{\alpha}\frac{\left(\sigma/\rho\right)^{0.6}}{\epsilon^{0.4}}\left(\frac{\mu_b}{\mu}\right)^{0.25} + C_2 \tag{8}$$

where α is the volume fraction of bubbles, σ is the surface tension and ϵ is the turbulent energy dissipation. For the model coefficients we assume $C_1 = 4.0$ (typical for bubbles in liquids) and $C_2 = 200\ \mu$m (smallest expected bubble size). For further details, including time scale for coalescence or break up, refer to Laux and Johansen [17].

The bubble (i.e. gas) density and its derivatives is governed by the compressibility of gas (i.e. pressure dependence). Since bubbles normally rise in water towards a lower hydrostatic pressure, we frequently describes this as gas expansion. The gas density is a function of pressure and for moderate depths we apply the ideal gas law

$$\rho_b = \frac{M_b p}{RT} \tag{9}$$

Here p is pressure, M_b is molecular weight of gas in bubble, R is the gas constant and T is temperature. For deeper plumes (typically below 200 meters) higher order correlations are required.

The motion of the bubbles is coupled to the flow of the background fluid. The background fluid is a liquid with a gas on top as illustrated in Figure 1. The bubbles are removed upon entering the gas phase. An Eulerian VOF method conserving mass and momentum through the Navier-Stokes equations is deployed to calculate the flow of the continuous background phases [18]. The interface between the continuous liquid and gas phases are tracked by the GEO reconstruct scheme [19]. The coupling with the Lagrangian bubbles is achieved through a source term in the momentum equation accounting for bubble drag

$$\rho \frac{D\mathbf{U}}{Dt} = \rho \boldsymbol{g} - \nabla p + \nabla \cdot [\mu_{\text{eff}}(\nabla \boldsymbol{U} + \nabla \boldsymbol{U}^T)] + \boldsymbol{S}_b \tag{10}$$

where μ_{eff} is the effective viscosity (molecular + turbulent) and S_b is the source term due to drag of bubbles

$$\boldsymbol{S}_b = \sum \frac{18\mu C_D \text{Re}}{24\rho_b d_b^2}(\boldsymbol{u}_b - \boldsymbol{u})\dot{m}_b \frac{\Delta t}{\Delta V_c} \tag{11}$$

Here Δt is the time step and ΔV_c is the volume of the computational cell. Turbulence and turbulent viscosity is accounted for by the standard k-ϵ model [20] or with the VLES model described below. Turbulence is damped at the interface between the continuous liquid phase and the gas phase above because turbulent structures are not carried through the interface. This is not inherently accounted for by VOF models since the interfaces are not treated as boundaries. Thus a source term in the dissipation equation for turbulence is added to increase dissipation and dampen turbulence at the interface [21].

Bubbles causes velocity fluctuations in the liquid due to the shedding of vortices behind the bubbles. These flow structures further interact with turbulent flow structures produced by the large scale flow. The result of these processes is that the turbulence structure is modified by the bubbles, resulting in bubble induced or bubble modified turbulence. Bubble induced turbulence is currently not accounted for by the model. Depending on the conditions, bubble induced turbulence could either increase or decrease plume spreading. Bubble induced turbulence can be accounted for by adding a term to the viscosity or by adding source terms in the differential equations for turbulent kinetic energy and turbulent dissipation [3, 22, 23]. The latter approach has recently been established as the most appropriate method. It does however need a model for the timescale of dissipation due to the bubbles, and several models for the timescale have been suggested. Several scientists claim to have identified the correct timescale model, but there is little agreement and consistency between the different scientists. As pointed out by Schwarz [22], the current timescale models seems to be an adjustable parameter depending on flow conditions. Thus, we have decided not to include bubble induced turbulence in this work.

2.1 VLES model

Modelling turbulence by a RANS approach (e.g. k-ϵ model) is quite common in engineering computations of turbulent flows. The models are robust and computationally affordable, but have some well-known deficiencies for transient flows. LES modelling is an alternative, but is computationally quite expensive. By introducing a filter in an unsteady RANS approach Johansen, Wu and Shyy [5] developed an affordable transient turbulence model. The model is designed to resolve dynamically the turbulent structures with physical extent above a given filter size. This is done by applying a top-hat filter to the momentum equations. The sub filter turbulence is accounted for by solving the transport equation for the sub filter energy (non-resolved flow). The turbulent stresses caused by the sub filter

flow is modeled, similar to a RANS computation, but where the turbulent viscosity is a result of filter length scale and sub filter turbulent energy. In this way, the model dynamically resolves the larger flow structures, and the major contributions to mixing, dispersion and momentum exchange are reproduced by the resolved flow. One major advantage with this approach, compared to standard RANS modeling, is that gravity effects due to density gradients (buoyancy, thermal or compositional stratification) is treated by the resolved model and thereby makes the model less vulnerable to the accuracy of closures for these specific effects. The turbulence model is known as a VLES (very large eddy simulation) model and has later been adopted by others, e.g. Labois and Lakehal [24].

The VLES model filters out the velocity fluctuations caused by turbulent structures above a given filter size Δ (i.e. below the corresponding wave number κ_Δ)

$$u'_\Delta = \sqrt{\frac{2}{3}k_\Delta} = \int_{\kappa_\Delta}^{\infty} \Phi(\kappa)\, d\kappa \tag{12}$$

where κ is the wave number of the Kolmogorov equilibrium spectrum for isotropic rms velocities

$$\Phi(\kappa) = \frac{1}{3} C_K^{1/2} \kappa^{-1/3} \epsilon^{1/3} \tag{13}$$

The cut-off wave number is linked to the filter size Δ by

$$\kappa_\Delta = \frac{2\pi}{\Delta} \tag{14}$$

Combining Eqs.12-14 yields

$$u'_\Delta = \pi^{-1/3}\, C_K^{1/2}\, \epsilon_\Delta^{1/3} \Delta^{1/3} \tag{15}$$

From this expression we see that the velocity fluctuations captured by the turbulence model increases as the filter size increases since more of the turbulence is maintained by the sub-filter model.

An expression for the turbulent viscosity can be derived from its definition

$$\nu_t = \langle u'_\Delta \cdot l_t \rangle = \int_{\kappa_\Delta}^{\infty} \Phi(\kappa) \frac{2\pi}{\kappa}\, d\kappa \tag{16}$$

where l_t is the turbulent length scale, and by acknowledging that the largest effective length scale is limited by the effective length scale of the sub-filter model. For a k-ϵ model the length scale is

$$l_{\text{eff}} = C_\mu \sqrt{\frac{3}{3}} k^{3/2} \epsilon^{-1} \tag{17}$$

with $C_\mu = 0.09$ for the standard k-ϵ model [20]. This leads to the following expression for the kinematic turbulent viscosity [5]

$$\nu_t = C_\mu \frac{k_\Delta^2}{\epsilon_\Delta} \cdot \mathrm{MIN}\left[1\,;\ \frac{\Delta\,\epsilon_\Delta}{k_\Delta^{3/2}}\right] \tag{18}$$

We see that for large filter sizes the turbulent viscosity is given by the sub-filter model. With a standard k-ϵ model as the sub-filter model, the VLES model is defined by Eq.12 and the partial differential equations for kinetic energy and energy dissipation of the k-ϵ model. Further details are given by Johansen, Wu and Shyy [5]. We apply the grid size as the filter size Δ. Thus for coarse grids most of the turbulence is maintained by the sub-filter model (u'), and for finer grids more of the turbulence is maintained within the velocity field governed by the momentum equations (U).

In order to apply the VLES model in an Eulerian-Lagrangian modelling framework an expression for the eddy time scale is required for the random walk model, i.e. Eq.(5) needs to be modified.

Eddy lifetime for non-resolved turbulence is defined by

$$\nu_\mathrm{t} = \langle {u'_\Delta}^2 \rangle \cdot \tau_{e_\Delta} \tag{19}$$

Combining this with Eqs.14 and 18 we can express the non-resolved Lagrangian time scale by

$$\tau_{\mathrm{e}_\Delta} = \frac{3}{2}\frac{\nu_\mathrm{t}}{k_\Delta} = \frac{3}{2} C_\mu \frac{k_\Delta}{\epsilon_\Delta} \cdot \mathrm{MIN}\left[1\,;\ \frac{\Delta\,\epsilon_\Delta}{k_\Delta^{3/2}}\right] \tag{20}$$

The subindex Δ in the above equation indicates that the kinetic energy and dissipation is based on the turbulent energy residing within the length scales of the filter. More details and full derivation of the VLES model is provided by Johansen and Shyy [6].

The modelling concept is implemented in ANSYS/Fluent 15.0. The PISO scheme is applied for pressure-velocity coupling, spatial discretization are second order or higher and the time discretization is implicit first order. The PISO scheme is normally robust with fast convergence.

3 RESULTS

The above modelling concept has been applied to a series of gas releases from 50 meters depth. This is equivalent to the cases presented in the experimental study of Milgram [25] who released air at gas rates of 0.03, 0.14, 0.34 and 0.71 kg/s in a sinkhole in Florida. The air was released through an upwardly directed pipe with an internal diameter of 5 cm. In the model simulations, the gas was released through a circular area with a diameter of 5 cm and with an injection velocity corresponding to the gas rates and release area. The computational grid was constructed from a coarse uniform grid which was refined 5 times towards the center of the plume as described by Olsen and Skjetne [12] with a center resolution of 8 cm. Thus, the flow in the release zone is not resolved. As a consequence of this the bubble size close to the release zone is not based on the flow predictions, but on an empirical jet model [26]. For contemplations on length scales it should be noted that the Kolmogorov length scale varies between 3 mm and 5 cm in the plume, the subgrid turbulent length scale is between 5 cm and 1 meter inside the

plume and up to 50 meters in the water outside the plume and the local mean bubble size is roughly 3-5 mm.

The bubble plumes achieved after a quasi-steady state is reached are shown in Figure 2. Results for both VLES and k-ϵ turbulence models are compared. We see how the results with the k-ϵ model reflect the averaged nature of the turbulence model with clear cone shaped plumes. The plume shapes of the VLES model include turbulent structures typically observed in experiments. Turbulent structures are also seen in Figure 3 where velocity contours are plotted on an iso-surface defined by vorticity. The observations of turbulent structure and dynamics in the VLES simulations do not necessarily prove that the VLES model is superior, as a time average of the VLES model might result in the same plume shapes as for the k-ϵ model. Figure 4 illustrates the difference between a time-averaged and instantaneous velocity field from the VLES model compared with the k-ϵ model. The time-averaged velocities for the VLES compare reasonably to the k-ϵ model results. We note that a snap shot of the flow and the time averaged result from the VLES model are quite different. The width of the plume may thus seem smaller for the VLES than the k-ϵ simulations when looking at the snap shot (e.g. Figure 2), whereas the time averaged plume might be wider.

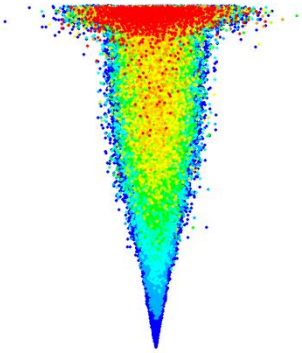

k-ϵ model at $\dot{m}$=0.03 kg/s

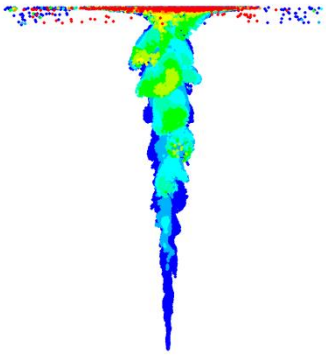

VLES model at $\dot{m}$=0.03 kg/s

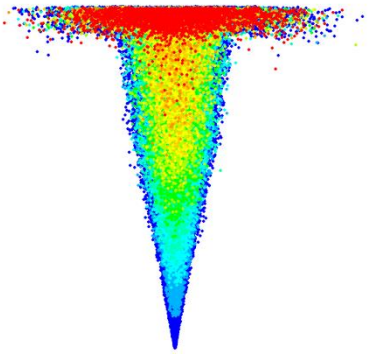

k-ϵ model at $\dot{m}$=0.14 kg/s

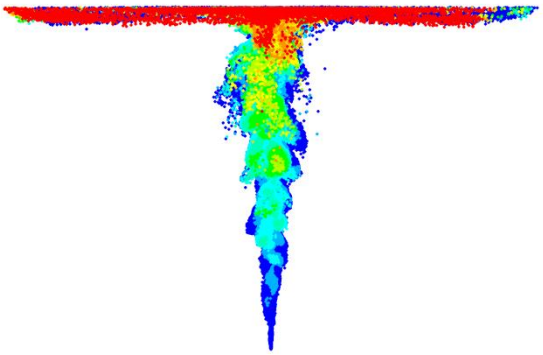

VLES model at $\dot{m}$=0.14 kg/s

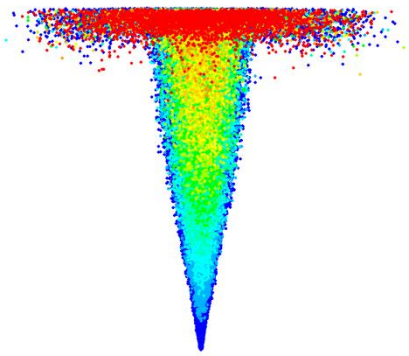

k-ϵ model at $\dot{m}$=0.34 kg/s

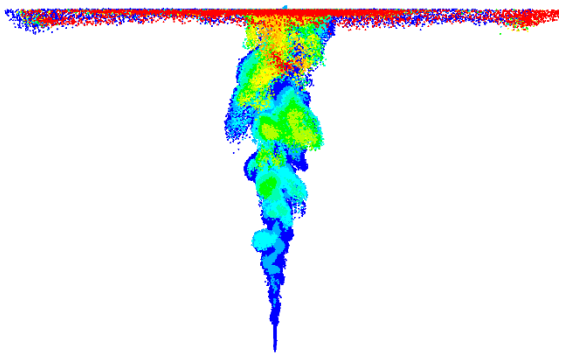

VLES model at $\dot{m}$=0.34 kg/s

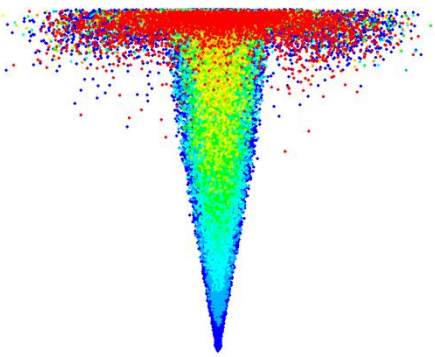

k-ϵ model at $\dot{m}$=0.71 kg/s

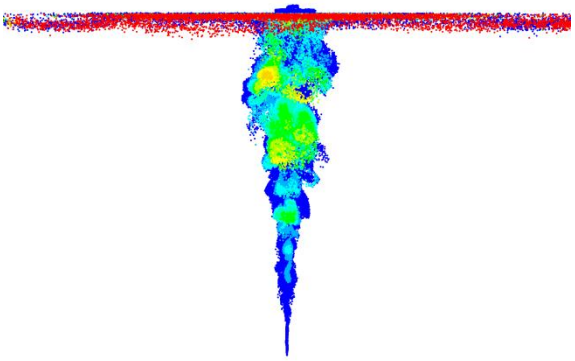

VLES model at $\dot{m}$=0.71 kg/s

Figure 2: Plume shapes colored by bubble distance out of the image plane for different gas rates and turbulence models. Blue equals 0 meter and red equals 8 meters.

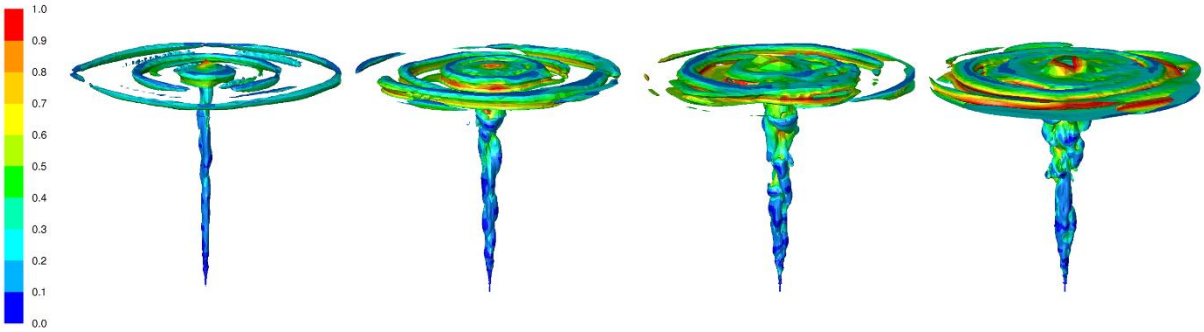

Figure 3: Contours of velocity magnitude (m/s) on iso-surfaces of vorticity magnitude of 0.5 for gas rates of 0.03, 0.14, 0.34 and 0.71 kg/s (left to right).

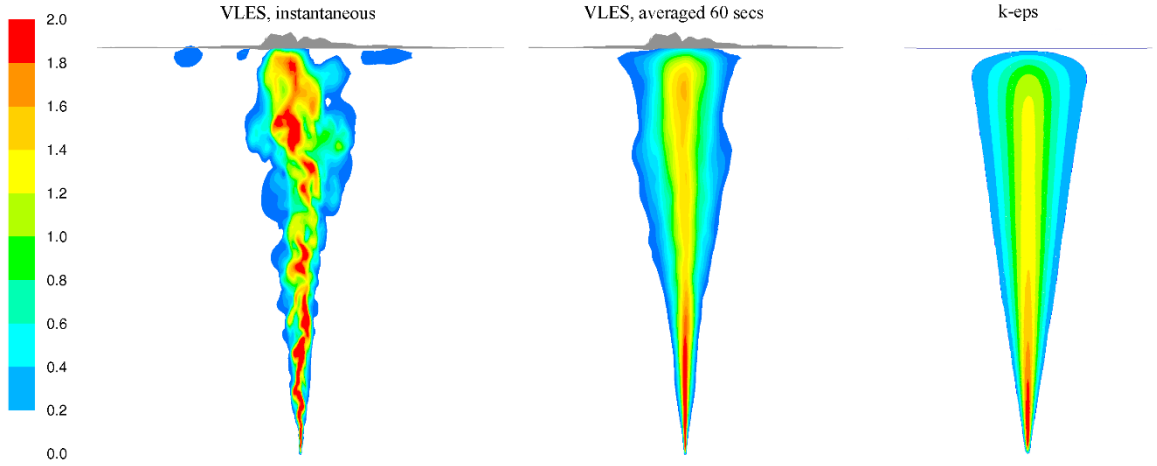

Figure 4: Contours of vertical velocity (m/s) through the plume center plane for a gas rate of 0.71 kg/s.

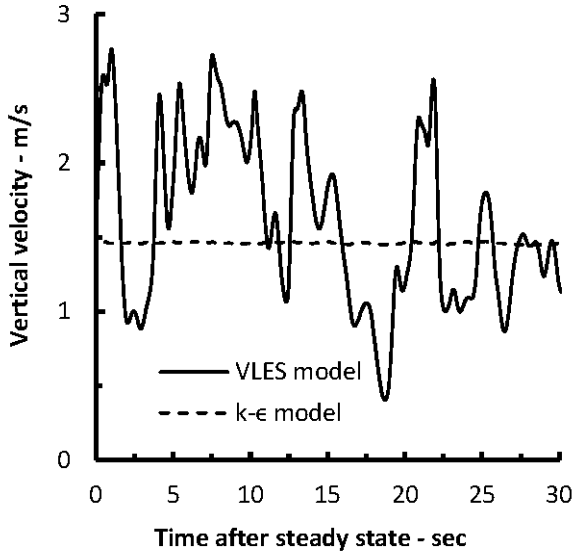

Figure 5: Vertical velocity 25 meters above release point at an arbitrary time period after steady state is established.

Qualitatively we see that the VLES model resolves more of the turbulent structures than the k-ϵ model. This is also confirmed by Figure 5 where the vertical velocity midway between release source and water surface is plotted. The k-ϵ model produces a typical averaged velocity plot with very small fluctuations. The VLES model reproduces the larger velocity fluctuations as expected from this kind of turbulence model. This indicates that some kind of averaging should be considered before reporting the results from the VLES simulations. Figure 6 show the vertical water velocity along the plume center from the seabed to the surface with different averaging periods. Not surprisingly, the instantaneous velocity profile from the VLES model is quite fluctuating while the profile from the k-ϵ model is quite smooth. An average over 10 secs. for the VLES results shows significant smoothing of the velocity profile. This is consistent with Figure 5, which indicates that multiple fluctuations are captured within a time frame of 10 seconds. Longer averaging periods smooths the profiles further. No significant extra smoothing is seen when extending the averaging from 50 to 60 secs. Thus 60 secs. is applied as the averaging period for reporting of VLES results. The effect of averaging is also seen in Figure 7 where volume fraction of gas bubbles is plotted. The randomness in the volume fraction for the k-ϵ model is caused by the random walk model for the bubble motion. Note that the volume fraction drops steeply in the region close to the release zone, and that the VLES model predicts a lower volume fraction than the k-ϵ model.

Another difference in the modelling approach of turbulence is the prediction of eddy viscosity. Since most of the turbulent spectrum is handled by the turbulence model in the k-ϵ approach and much less in the VLES approach, higher values of eddy viscosity is expected in the k-ϵ approach. This is confirmed by the simulation results plotted in Figure 8. The k-ϵ model obtains a much higher eddy viscosity than the VLES model. Note also that the eddy viscosity from the VLES model is hardly affected by the gas rate, whereas the eddy viscosity from the k-ϵ model strongly depends on the gas rate. The peak in eddy viscosity close to the surface for the k-ϵ simulations is a well known anomaly as turbulence is overpredicted close to stagnation points [27].

The model results can also be compared quantitatively with the experimental results of Milgram [25]. Milgram measured velocities at different heights above the release source and fitted the measurement to Gaussian velocity profiles

$$U(z,r) = U_c(z) \cdot \exp(-r^2/b(z)^2) \tag{21}$$

where the plume radius, b, and the axis velocity, U_c,, varies with distance, z, above the release source. Velocity profiles where measured at 6 heights above the release source. Axial velocity and plume radius was reported based on curve fit between the expression above and the experimental results averaged over 10 minutes. Plume radius can also be extracted from the model simulations. A comparison is seen in Figure 9 for a gas rate of 0.71 kg/s. Both k-ϵ and VLES model underpredict the plume spreading somewhat, and the k-ϵ model underpredicts most.

By defining a plume angle based on the plume radius at the second highest profile height, $\alpha = \mathrm{atan}(b_{43.9}/43.9)$, quantitative comparisons are made between experiments and the two turbulence models. The results are seen in Figure 10. We see that the k-ϵ model do not capture the trend of the experimental values. The VLES model captures the trend, but underpredicts the plume angle by roughly 10-15%. The deviation between the VLES model and the experiments are smaller at the lower gas rates. The deviation is acceptable considering the complexity of the phenomenon. Attempts towards closing the deviation should still be considered. Two possible causes for the deviation are failure to capture all relevant physics in the model and flaws in the experimental measurements.

With respect to the experimental measurements [25], it should be noted that the velocity profiles were obtained by current meters based on a propeller concept. It is not mentioned whether flow direction was recorded and/or accounted for. The turbulence in a bubble plume will cause the flow to move upwards

with circulating fluctuations. These fluctuations may periodically result in a downward flow. If this is not accounted for, the reported averaged velocity profiles will be wider than the true velocity profiles.

The above mentioned results deal with conditions in the water column. Conditions at the surface are also of interest, especially for those concerned about the safety of surface operations. In Figure 11 contours of the surface velocities is seen at the water/air-interface. The velocity and the extent of the influenced zone increases with increasing gas release rate. This was also observed experimentally [28].

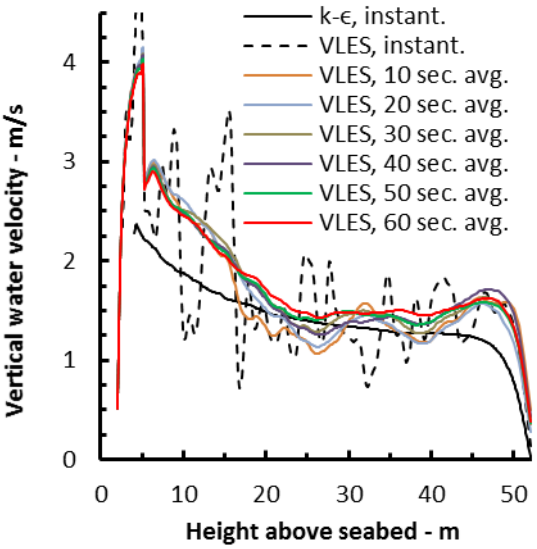

Figure 6: Vertical water velocity for a gas rate of 0.71 kg/s as function of height above the seabed along the plume axis for the k-ϵ model and for the VLES model.

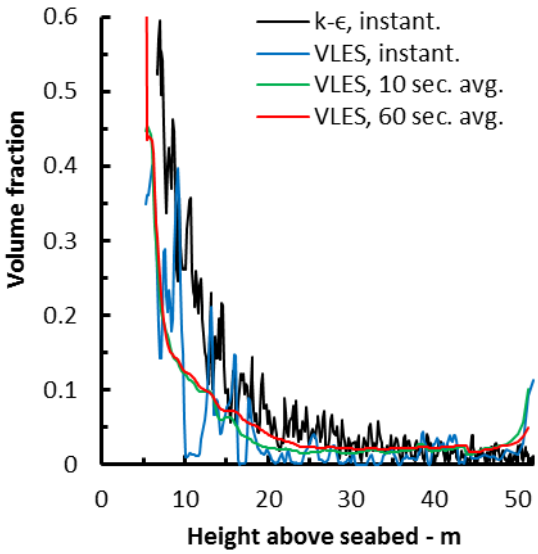

Figure 7: Gas volume fraction for a gas rate of 0.71 kg/s as function of height above the seabed along the plume axis for the k-ϵ model and for the VLES model.

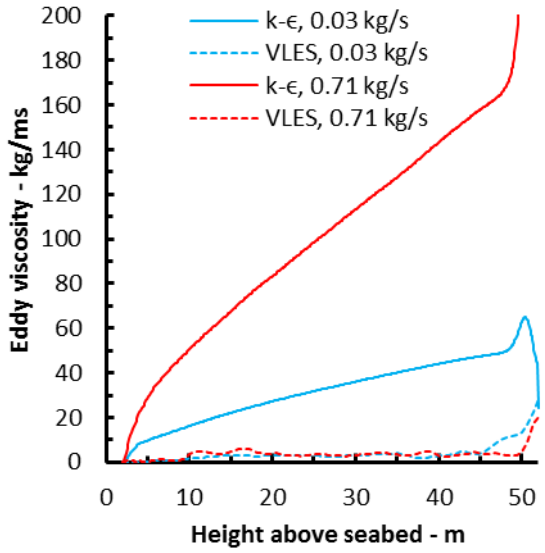

Figure 8: Eddy viscosity for lowest and highest gas rate of 0.71 kg/s as function of height above the seabed along the plume axis for the k-ϵ model and the VLES model. Instantaneous values are presented.

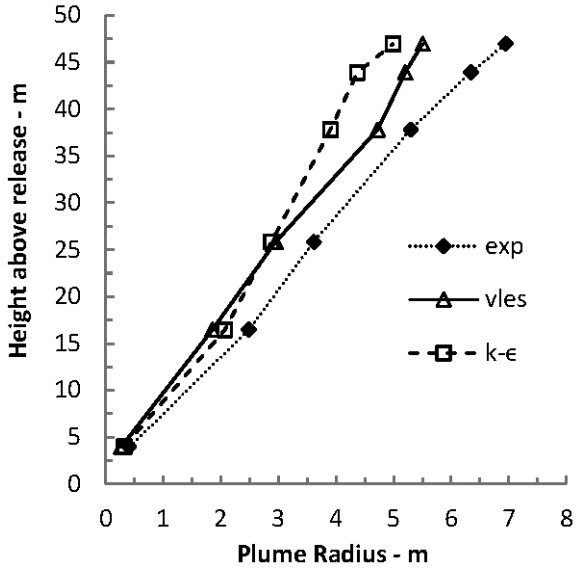

Figure 9: Plume radius vs height above release source for a gas rate of 0.71kg/s.

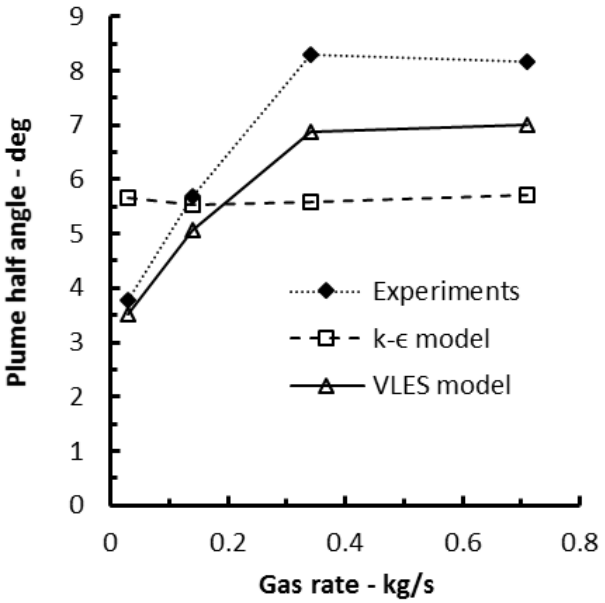

Figure 10: Plume half angle as function of gas rate.

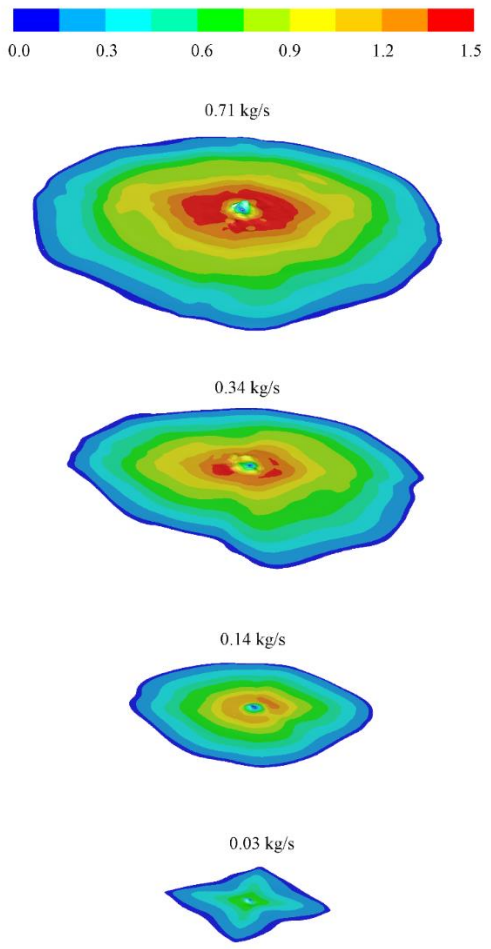

Figure 11: Contours of radial surface velocities (m/s) limited to 0.1 m/s and above.

4 SUMMARY AND DISCUSSION

An Eulerian-Lagrangian modelling concept for bubble plumes has been presented. A VLES turbulence model has been introduced into the modelling concept. When compared to a k-ϵ model, the VLES model captures more of the turbulence spectrum inherently and leaves less of the spectrum to the model assumptions of the sub-filter turbulence model. When comparing the model with experimental results of a series of gas discharges in a sinkhole from a depth of 50 meters, we find that the VLES model is more consistent with the experimental observations than the k-ϵ model.

Although the VLES model is preferable over the k-ϵ model, it should be noted that the VLES underpredicts plume spreading somewhat. This is not surprising since bubble induced turbulence and lift forces are currently not accounted for in the modelling concept. Both of these mechanisms will normally create more spreading of the plume, although in some circumstances spreading might also be reduced. It should also be mentioned that the experimental method may have caused an over-assessment of the plume angle. Future efforts will focus on bubble induced turbulence, the lift force and comparison with other experimental results.

ACKNOWLEDGEMENT

This study was performed within the SURE-project (phase II) supported by Gassco, Statoil, Total, Safetec, Wild Well Control and Petroleum Safety Authority Norway.

The paper is an extended version of a conference paper presented at the Eleventh International Conference on CFD in the Minerals and Process Industries (CFD2015). The paper was invited by the conference organizers for submission to the CFD2015 Special Issue of Applied Mathematical Modelling.

REFERENCES

[1] B.R. Morton, G.I. Taylor, J.S. Turner, Turbulent gravitational convection from maintained and instantaneous sources, Proc.Roy.Soc.A, 234 (1956) 171-178.
[2] M.P. Schwarz, W.J. Turner, Applicability of the standard k-ϵ turbulence model to gas-stirred baths, Applied Mathematical Modelling, 12 (1988) 273-279.
[3] S.T. Johansen, F. Boysan, Fluid Dynamics in Bubble Stirred Ladles: Part II. Mathematical Modelling, Metallurgical Transcations B, 19B (1988) 756-764.
[4] C. Swan, A. Moros, The hydrodynamics of a subsea blowout, Appl Ocean Res, 15 (1993) 269-280.
[5] S.T. Johansen, J. Wu, W. Shyy, Filter-based unsteady RANS computations, Heat and Fluid Flow, 25 (2004) 10-21.
[6] S.T. Johansen, W. Shyy, Turbulence modeling using RANS models with a pre-defined filter size, SINTEF report A27886 (open to public), 2016.
[7] B. Niceno, M.T. Dhotre, N.G. Deen, One-equation sub-grid scale (SGS) modelling for Euler-Euler large eddy simulation (EELES) of dispersed bubbly flow, Chemical Engineering Science, 63 (2008) 3923-3931.
[8] M.V. Tabib, S.A. Roy, J.B. Joshi, CFD simulation of bubble column - An analysis of interphase forces and turbulence models, Chem Eng J, 139 (2008) 589-614.
[9] M.V. Tabib, P. Schwarz, Quantifying sub-grid scale (SGS) turbulent dispersion force and its effect using one-equation SGS large eddy simulation (LES) model in a gas-liquid and a liquid-liquid system, Chemical Engineering Science, 66 (2011) 3071-3086.
[10] D. Zhang, N.G. Deen, J.A.M. Kuipers, Numerical simulation of the dynamic flow behavior in a bubble column: A study of closures for turbulence and interface forces, Chemical Engineering Science, 61 (2006) 7593-7608.
[11] M.E. Díaz, F.J. Montes, M.A. Galan, Influence of the lift force closure on the numerical simulation of bubble plumes in a rectangular bubble column, Chem.Eng.Sci., 64 (2009) 930-944.
[12] J.E. Olsen, P. Skjetne, Modelling of underwater bubble plumes and gas dissolution with an Eulerian-Lagrangian CFD model, Appl Ocean Res, 59 (2016) 193-200.
[13] A.D. Gosman, E. Ioannides, Aspects of computer simulation of liquid-fuelled combustors, J.Energy, 7 (1983) 482-490.
[14] A. Tomiyama, I. Kataoka, I. Zun, T. Sakaguchi, Drag coeffcients of single bubbles under normal and micro gravity conditions, JSME International Journal, Series B, 41 (1998) 472-479.
[15] Y. Tsuji, Y. Morikawa, K. Terashima, Fluid-dynamic interaction between two spheres, Int.J.Multiphase Flow, 8 (1982) 71-82.
[16] A. Tomiyama, A. Tamai, H. Zun, S. Hozokawa, Transverse migration of single bubbles in simple shear flows, Chem.Eng.Sci., 57 (2002) 1849-1858.
[17] H. Laux, S.T. Johansen, A CFD analysis of the air entrainment rate due to a plunging steel jet combining mathematical models for dispersed and separated multiphase flows, Fluid Flow Phenomena in Metals Processing, 1999, pp. 21-30.
[18] C.W. Hirt, B.D. Nichols, Volume of fluid (VOF) method for the dynamics of free boundaries, Journal of Computational Physics, 39 (1981) 201-225.
[19] D.L. Youngs, Time-Dependent Multi-Material Flow with Large Fluid Distortion, in: K.W. Morton, M.J. Banes (Eds.) Numerical Methods for Fluid Dynamics, Academic Press1982.
[20] B.E. Launder, D. Spalding, The numerical computation of turbulent flows, Computer methods in applied mechanics and engineering, 3 (1974) 269-289.
[21] Q.Q. Pan, J.E. Olsen, S.T. Johansen, M. Reed, L. Sætran, CFD Study of Surface Flow and Gas Dispersion From a Subsea Gas Release ASME 2014 33rd International Conference on Ocean, Offshore and Arctic EngineeringSan Francisco, 2014.
[22] M.P. Schwarz, Bubble induced turbulence in two-fluid simulation if bubbly flow, 26th International Symposium on Transport PhenomenaLeoben, Austria, 2015.
[23] R. Rzehak, E. Krepper, Bubble-induced turbulence: Comparison of CFD models, Nuclear Engineering and Design, 258 (2013) 57-65.

[24] M. Labois, D. Lakehal, Very-Large Eddy Simulation (V-LES) of the flow across a tube bundle, Nuclear Engineering and Design, 241 (2011) 2075-2085.
[25] J.H. Milgram, Mean flow in round bubble plumes, Journal of Fluid Mechanics, 133 (1983) 345-376.
[26] L. Zhao, M.C. Boufadel, S.A. Socolofsky, E. Adams, T. King, K. Lee, Evolution of droplets in subsea oil and gas blowouts: Development and validation of the numerical model VDROP-J, Marine Pollution Bulletin, 83 (2014) 58-69.
[27] W.C. Strahle, stagnation point flows with freestream turbulence - the matching condition, AIAA J., 23 (1985) 1822-1824.
[28] J.H. Milgram, J.J. Burgess, Measurements of the surface flow above roudn bubble plumes, Appl Ocean Res, 6 (1984) 40-44.